



**HAL**  
open science

# Influence of atmosphere on high-temperature oxidation of Fe-Cr-Si model alloy

Christophe Issartel, H. Buscail, Stéphane Mathieu

► **To cite this version:**

Christophe Issartel, H. Buscail, Stéphane Mathieu. Influence of atmosphere on high-temperature oxidation of Fe-Cr-Si model alloy. *Materials and Corrosion / Werkstoffe und Korrosion*, 2019, 70 (8), pp.1410-1415. 10.1002/maco.201810579 . hal-02303179

**HAL Id: hal-02303179**

**<https://uca.hal.science/hal-02303179>**

Submitted on 2 Oct 2019

**HAL** is a multi-disciplinary open access archive for the deposit and dissemination of scientific research documents, whether they are published or not. The documents may come from teaching and research institutions in France or abroad, or from public or private research centers.

L'archive ouverte pluridisciplinaire **HAL**, est destinée au dépôt et à la diffusion de documents scientifiques de niveau recherche, publiés ou non, émanant des établissements d'enseignement et de recherche français ou étrangers, des laboratoires publics ou privés.

**Title:** Influence of atmosphere on high temperature oxidation of Fe-Cr-Si model alloy

C. Issartel\*, H. Buscail, S. Mathieu

*Issartel*

LVEEM, 8 rue J.B. Fabre, 43000 Le Puy en Velay/France.  
christophe.issartel@uca.fr

*Buscail*

LVEEM, 8 rue J.B. Fabre, 43000 Le Puy en Velay/France.

*Mathieu*

IJL - UMR 7198, CNRS, Université de Lorraine, Campus ARTEM, 2 allée André Guinier,

BP 50840, 54011 Nancy/France

**Abstract.** The aim of this work is to show the influence of the gaseous environment on the ferritic Fe-Cr-Si model alloy oxidation during 70 h, at 900 °C and 950 °C. Two different atmospheres have been used: air or nitrogen containing 5 Vol.% hydrogen (N<sub>2</sub>-5%H<sub>2</sub>).

After air oxidation, a non-adherent chromia scale formed. In the N<sub>2</sub>-5%H<sub>2</sub> gaseous environment, it clearly appears that silicon segregation near the internal scale-metal interface is favoured. In this low oxygen containing gas, adherent chromia and silica scales have been formed. Silica subscale associated to an adherent chromia scale obtained in low oxygen conditions are a good protection barrier against carburisation.

Keywords: chromia, silica, ferritic alloy, high temperature oxidation, N<sub>2</sub>-5 vol.% H<sub>2</sub>

## 1 Introduction

Many alloys are used in high-temperature carburising and nitriding conditions. These environments induce severe degradation and leads to the weakening of the alloy. To improve the alloy carburisation and nitriding resistance, it is considered that the presence of an adherent oxide scale acts as a diffusion barrier. On chromia-forming alloys, the oxidation leads to a chromia scale and this scale acts as a good diffusion barrier based on the assumption that oxidation occurs under isothermal conditions. [1] Nevertheless, cyclic oxidation can lead to the chromia scale spallation. To better improve the alloy protection, it has also been proposed that silicon can be beneficial against carburisation in promoting a protective silica scale formation. [2,3] Then chromia-forming alloy with additional silicon are used. However, former studies have shown that the oxidation in air leads to a poorly adherent chromia scale and did not permit a continuous silica scale formation even though the alloy contains about 2 wt% silicon. [4-6] One way to act on the oxide scale formation consists of modifying the gaseous environment, using inert gases. [7] Previous works have shown that, on an austenitic steel, a protective silica-scale formation is promoted by low-oxygen gaseous environments and a high alloy silicon content. [8] Based on what is known about the oxidation behaviour of this austenitic steels, this work will focus on the influence of a low-oxygen-potential gaseous environment on a ferritic alloy oxidation during 70 h, at 900 and 950 °C. The low-oxygen-potential gaseous environment used,  $N_2$ -5% $H_2$ , simulates industrial conditions encountered in the heat treatment furnaces. Previous works performed in  $N_2$ -5% $H_2$  atmosphere has shown nitridation of pure chromium. These authors explained that, at 950 °C,  $Cr_2N$  and  $CrN$  are the stable nitrides at high  $pN_2$  and low  $pO_2$  environments. [9] Another work has shown that the presence of silicon modifies the stability of oxides and nitrides. [10] Results showed that 3 at% silicon addition with chromium significantly improved the oxidation and nitridation resistance. The present work does not deal about pure chromium oxidation but particular attention is paid to the evolution of nitride phases during oxidation.

The aim of our work is to investigate the formation of a silica scale formed on a ferritic model alloy with low-oxygen-containing gaseous environments compared to oxidation in air.

## **2 Materials and methods / Experimental**

The material used in the present work is a model Fe-Cr-Si made by “Surface et Interface, Réactivité Chimique des Matériaux (SIRCM)” of institute “jean Lamour” of Nancy. The alloy was prepared by high-frequency melting according to the following composition: 71.5%wt (68.8 at.%) of iron, 26.45%wt (27.3 at.%) of chromium and 2.05%wt (3.9 at.%) of silicon. Bulk elements with purities higher than 99.95% were placed into a water-cooled copper crucible and then enclosed in a silica tube. Prior to each experiment, three to four sequences of vacuuming and argon filling were performed in order to clean the atmosphere of the reactor. To avoid significant volatilisation of the metallic elements, the melting was conducted under argon with the pressure of 0.8 atm. The samples were re-melted three times to ensure a homogeneous element distribution. Finally, the samples were gravity casted in a cold copper mould to obtain ingots with the diameter of 10 mm. One-mm-thick cylindrical specimens of around 1.7 cm<sup>2</sup> total surface area were cut from the metallic bars. The specimens were abraded up to the 1200-grit SiC paper, then degreased with acetone and finally dried.

The kinetic results obtained under isothermal conditions were recorded during 70 h at 900 or 950 °C, in flowing (8 l/h) nitrogen containing 5 vol.% hydrogen (N<sub>2</sub>-5%H<sub>2</sub>) or air, using a Setaram TG-DTA 92–1600 microthermobalance. The residual pO<sub>2</sub> = 15 ppmv contained in the N<sub>2</sub>-5 vol% H<sub>2</sub> was measured by an oxygen analyser (Elcowa GPR1200MS). Thermogravimetric analyses have been performed 2 times on separate specimens to verify the reproducibility.

The oxide characterisation was realised by X-ray diffraction (XRD). XRD patterns were obtained by use of a Philips X'pert MPD diffractometer (copper radiation,  $\lambda_{k\alpha} = 0.15406$  nm). The XRD patterns were registered during 8h using a  $0.02^\circ$  step size, the  $2\theta$  is ranging from  $18^\circ$  to  $68^\circ$  and 12 s is the counting time. The oxide scale surface and cross section morphologies have been observed in a JEOL 7600 scanning electron microscope (SEM) coupled with a LINK energy dispersive X-ray spectroscopy (EDXS). The EDXS point analyses were performed with an electron probe focused to a  $1\text{-}\mu\text{m}$  spot.

### 3 Results

#### 3.1 Kinetics

Mass gain per unit area versus time curves ( $\Delta m/A = f(t)$ ) of specimens oxidised during 70 h at  $900^\circ\text{C}$ , in air and in  $\text{N}_2\text{-}5\text{ Vol}\% \text{H}_2$ , are reported in Figure 1. Similar curves concerning samples oxidized at  $950^\circ\text{C}$  are reported in Figure 2. The comparison of the kinetic curves shows that the Fe-Cr-Si alloy has a higher weight gain during the oxidation in air than in  $\text{N}_2\text{-}5\% \text{H}_2$ . In the  $\text{N}_2\text{-}5\% \text{H}_2$  atmosphere oxidation is due to the presence of 15 ppm oxygen. The calculation of the parabolic rate constants, from the slope of ( $\Delta m/A = f(\sqrt{t})$ ), evidences that the oxidation behaviour was parabolic in the two atmospheres. [11] Parabolic rate constants are given in table1.

The comparison of oxidation rates obtained at  $900^\circ\text{C}$  and  $950^\circ\text{C}$ , in  $\text{N}_2\text{-}5\% \text{H}_2$ , shows that the weight gains are close to each other. In air, the weight gain obtained during oxidation at  $950^\circ\text{C}$  was higher than the weight gain obtained during oxidation at  $900^\circ\text{C}$ .

Observation of samples after the oxidation tests in air has shown some scale spallation. No spallation was observed after the tests performed in  $\text{N}_2\text{-}5\% \text{H}_2$ .

### **3.2 Scanning Electron Microscopy observations**

Scanning Electron Microscopy has permitted the observation of surfaces and cross sections of samples (Figure 3 to 5). Figure 3 shows that spallation is significant on the samples oxidised in air at both temperatures. In  $N_2$ -5% $H_2$ , scale spallation was not observed.

Figure 4 shows that the chromia scale structure is different depending on the atmosphere used. We can observe a more porous structure when the oxidation atmosphere is performed in  $N_2$ -5% $H_2$ . The chromia grain size registered after oxidation at 900 °C is smaller than the one observed at 950 °C in air. The observed porosity in the scale formed in  $N_2$ -5% $H_2$  is also smaller when the oxidation temperature was 900 °C.

Figure 5 presents sample cross sections. The scale cross section morphology of the Fe-Cr-Si specimen oxidised in  $N_2$ -5% $H_2$  during 70 h at 900 °C (Fig. 5(b)) shows that a 1- $\mu$ m-thick oxide scale is present. EDXS analysis shows the presence of a chromia scale. A continuous silica layer is observed at the alloy/oxide interface. At the same temperature, the Fe-Cr-Si specimen oxidised in air during 70 h at 900 °C (Fig. 5(a)) show that a 3- $\mu$ m-thick chromia scale is present. No continuous silica scale is found and the chromia scale has spalled off from the substrate. Similar observations have been made on cross sections obtained after oxidation at 950 °C. A continuous silica layer is observed at the alloy/oxide interface in  $N_2$ -5% $H_2$  and a 1-1.5- $\mu$ m-thick chromia scale is present (Fig. 5(d)). In air, a 4- $\mu$ m-thick oxide scale is present, and the scale has spalled off to a less extent compared to 900 °C, (Fig. 5(c)).

### **3.3 X-Ray Diffraction analysis**

The oxide scale formed on the Fe-Cr-Si alloy after 70 h isothermal oxidation in N<sub>2</sub>-5%H<sub>2</sub> was analysed by XRD on the metallic substrate (Fig. 6). The substrate (ICDD 01-1262) and Cr<sub>2</sub>O<sub>3</sub> (ICDD 38-1479) are detected on the specimen surface. After oxidation in N<sub>2</sub>-5%H<sub>2</sub> the scale structures are similar at 900 and 950 °C. In air, the same phases are detected on the specimen's surface at 900 and 950 °C. Whatever the temperature or gaseous environment, no crystalline silica scale was detected by XRD.

## **4 Discussion**

### **4.1 Oxidation in air**

On a Fe-26Cr-2Si model alloy, the expected oxides are chromia Cr<sub>2</sub>O<sub>3</sub> or silica SiO<sub>2</sub> at 900 and 950 °C. Some authors proposed that the presence of nitrogen in air can also lead to nitride formation. At 950 °C, Dorcheh and al. have shown that Cr<sub>2</sub>N and CrN are the stable nitrides formed on pure chromium at high pN<sub>2</sub> and low pO<sub>2</sub>. [9] In the present work, the presence of crystalline phases was analysed by XRD. On Figure 6, our results indicate that only chromia was detected, and no nitrides were present. Kinetic results show that the weight gain obtained at 900 °C is smaller than the weight gain obtained at 950 °C. The chromia grain size is also smaller when the oxidation temperature is lower (Fig 4a, 4c). The weight gain curves are parabolic. This behaviour corresponds to a growth process limited by the diffusion through a continuous and growing scale acting as a diffusion barrier. According to Hussey, the transport mechanism in an oxide formed on a Fe-Cr alloy is predominantly limited by cation Cr<sup>3+</sup> diffusion. [12] This growth mechanism induces formation of cation vacancies and their coalescence at metal-oxide interface leads to cavities promoting the bad scale adherence. It corresponds to our results showing that, scale spallation occurred during cooling, after air

oxidation (see Fig 3a and 3c). According to other authors, silicon is supposed to be present as a silica film. [13-15] Then silica leads to a decrease of the alloy oxidation rate. [16] The high silicon affinity to oxygen, permit its internal oxidation, developing SiO<sub>2</sub> precipitates at the internal interface. [17,18] Then, silica acts as a diffusion barrier and pegs the chromia scale to the substrate. [19,20] In the present work, no silica film has been detected by SEM at the internal interface after oxidation in air, but some isolated silica grains can be observed on the cross sections (Fig. 5a, 5c). Moreover, it is proposed that a too high amount of silicon induces more scale spallation between the alloy and the silica scale or at the silica/chromia interface. [21] It is the reason why silicon is rarely added at more than 1 wt%. In our case, the silicon content is 2 wt%. This silicon content was chosen to be high enough to obtain a thick silica scale. Nevertheless, air oxidation does not lead to a silica scale formation at 900 and 950 °C.

#### **4.2 Oxidation in N<sub>2</sub>-5%H<sub>2</sub>**

Some works about oxidation in N<sub>2</sub>-5 %H<sub>2</sub> have been proposed. Dorcheh and al. used this gas at 950-1200 °C as purely nitriding atmosphere on pure chromium. [9] In our case, chromium is present as an alloying element and no nitrides have been observed by XRD or by EDS. The supposed reducing character of this atmosphere can explain the lack of literature, but this atmosphere contains 15 ppm O<sub>2</sub> that can lead to the alloy oxidation. Kinetic results (figure 1 and 2) show that during the Fe-Cr-Si oxidation at 900 or 950 °C in N<sub>2</sub>-5%H<sub>2</sub>, the presence of 15 ppm oxygen allows the chromium oxidation. This oxygen content is high enough to induce the substrate oxidation because thermodynamic data indicate that  $p(\text{O}_2) = 10^{-22}$  atmosphere is sufficient to oxidised chromium at 900 °C. According to the Ellingham diagram, thermodynamic data also indicate that  $p(\text{O}_2) = 10^{-30}$  atm. is enough to oxidised silicon at 900 °C. XRD results have shown that, the oxide scales are composed of Cr<sub>2</sub>O<sub>3</sub>. Even if XRD

results are similar between air and  $N_2-5\%H_2$ , SEM-EDS results have shown a silica subscale under the chromia scale (Fig 5b, 5d). On the XRD patterns, the metallic substrate was observed, then all the oxide scale thickness was analysed (Fig 6). The silica scale is not detected by XRD because it is an amorphous oxide. The major difference between oxidation in air and oxidation in  $N_2-5\%H_2$  is the presence of this silica subscale. The effect of silicon on the oxidation process has already been examined on chromia-forming alloys. It generally acts as a protective element. Even though too much silicon is considered as detrimental for the steel mechanical properties, its addition generally improves the oxidation resistance. [22] Some authors stated that silicon segregates at the oxide/alloy interface and blocks the iron cationic diffusion. [13-15] Silicon is then supposed to be present as a silica film, which lowers the steel oxidation rate. The effect of a low oxygen environment, at the alloy surface, can be related to other works describing the effect of surface coatings limiting the oxygen access to the alloy surface. [7] Some authors have shown that an yttrium sol-gel coating promotes a continuous silica scale formation at the internal interface on the alloy AISI 304 due to a limited access of the oxygen to the metallic surface. [16] Onishi has also calculated the conditions at the boundary between internal and external oxidations of Si-containing steels (Fe-Si alloys) at 850 °C. [23] This author has demonstrated that under low oxygen potential a very thin  $SiO_2$  layer forms on the alloy surface because the diffusion rate of silicon is relatively high compared with that of oxygen. It is then concluded that internal oxidation occurs in a restricted oxygen partial pressure range and is limited to silicon concentrations below 1 wt%. The oxygen partial pressure range, in which internal oxidation can occur, decreases with increasing silicon content. When the silicon content increases, external silicon oxidation should occur. In the present work, the high silicon containing Fe-Cr-Si alloy permits the formation of a silica scale on the alloys surface under low oxygen potentials. It is due to the relatively high diffusion rate of silicon compared with that of oxygen. Figure 4 shows

another difference between an oxidation in air and an oxidation in N<sub>2</sub>-5%H<sub>2</sub>. The chromia scale obtained in N<sub>2</sub>-5%H<sub>2</sub> is porous and adherent. If an initial formation of a silica scale on the alloy surface occurs in a restricted oxygen partial pressure, then chromium diffusion decreases and the chromia formed can be porous. An internal oxidation process also favours the chromia scale adherence. As proposed by Nguyen and al., the protection against carburising environments is insured by the silica subscale and a more adherent chromia scale. [2,3]

## 5 Conclusion

This work has shown the influence of N<sub>2</sub>-5%H<sub>2</sub> on the ferritic Fe-Cr-Si oxidation during 70 h, at 900 and 950 °C. The N<sub>2</sub>-5%H<sub>2</sub> gaseous environment was used to simulate industrial heat treatment conditions. Under low oxygen potential a SiO<sub>2</sub> layer forms on the alloy surface because the diffusion rate of silicon is relatively high compared with that of oxygen. On this ferritic steel, the protective silica scale formation is promoted by low oxygen partial pressures and the high silicon content. The low oxygen partial pressure also induces a change in the transport mechanism from predominantly cation to predominantly anion diffusion. Then a porous, and more adherent, chromia scale is formed. The protection against corrosives environments is then insured by the silica subscale and a more adherent chromia scale.

## 6 References

- [1] R. Stevens, *Oxid. Met.* **1979**, *13*, 353.
- [2] T.D. Nguyen, J. Zang, D.J. Young, *Oxid. Met.* **2014**, *81*, 549.
- [3] T.D. Nguyen, J. Zang, D.J. Young, *Oxid. Met.* **2015**, *83*, 575.

- [4] C. Issartel, H. Buscail, C. T. Nguyen and A. Fleurentin, *Mater. Corros.* **2010**, *61*, 929.
- [5] H. Buscail, C. Issartel, F. Riffard, R. Rolland, S. Perrier, A. Fleurentin and C. Josse, *Appl. Surf. Sci.* **2011**, *258*, 678.
- [6] H. Buscail, C. Issartel, C. T. Nguyen, S. Perrier and A. Fleurentin, *Mater. Tech.* **2010**, *98*, 209.
- [7] H. Buscail, C. Issartel, F. Riffard, R. Rolland, S. Perrier and A. Fleurentin, *Corr. Sci.* **2012**, *65*, 535.
- [8] H. Buscail, R. Rolland, F. Riffard, C. Issartel, C. Combe, P.F. Cardey, *Oxid. Met.* **2017**, *87*, 837.
- [9] A.S. Dorcheh, M. Schütze, M.C. Galetz, *Corros. Sci.* **2018**, *130*, 261.
- [10] A.S. Dorcheh, M.C. Galetz, *Oxid. Met.* **2015**, *84*, 73.
- [11] B. Pieraggi, *Oxid. Met.* **1987**, *27*, 177.
- [12] R.J. Hussey, M.J. Graham, *Oxid. Met.* **1996**, *45*, 349.
- [13] S. N. Basu and G. J. Yurek, *Oxid. Met.* **1991**, *36*, 281.
- [14] A. M. Huntz, *Mater. Sci. Eng.* **1995**, *A201*, 211.
- [15] H. E. Evans, D. A. Hilton, R. A. Holm, and S. J. Webster, *Oxid. Met.* **1983**, *19*, 1.
- [16] F. Riffard, H. Buscail, E. Caudron, R. Cueff, C. Issartel, and S. Perrier, *J. Mater. Sci.* **2002**, *37*, 3925.
- [17] M. Landkof, A. V. Levy, D. H. Boone, R. Gray, and E. Yaniv, *Corr. Sci.* **1985**, *41*, 344.
- [18] G. Aguilar, J. P. Larpin, and J. C. Colson, *Mém. étud. sci. Rev. métall.* **1992**, 447.
- [19] S. Seal, S. K. Bose, and S. K. Roy, *Oxid. Met.* **1994**, *41*, 139.
- [20] R. N. Durham, B. Gleeson, and D. J. Young, *Oxid. Met.* **1998**, *50*, 139.
- [21] F.H. Stott, G.C. Wood, J. Stringer, *Oxid. Met.* **1995**, *44*, 113.

[22] F. Armanet, J.H. Davidson and P. Lacombe, *Les aciers inoxydables*, Les éditions de Physique, Les Ulis France **1990**.

[23] T. Onishi, S. Nakakubo and M. Takeda, *Met. Trans.* **2010**, *51*, 482.

	Atmosphere	N <sub>2</sub> -5 Vol% H <sub>2</sub>	Air
$k_p$ (g <sup>2</sup> .cm <sup>-4</sup> .s <sup>-1</sup> )	900 °C	$9 \times 10^{-8}$	$4.9 \times 10^{-7}$
	950 °C	$1.6 \times 10^{-7}$	$1.21 \times 10^{-6}$

**Table 1.** Parabolic rate constants of specimen oxidized at 900 °C and 950 °C

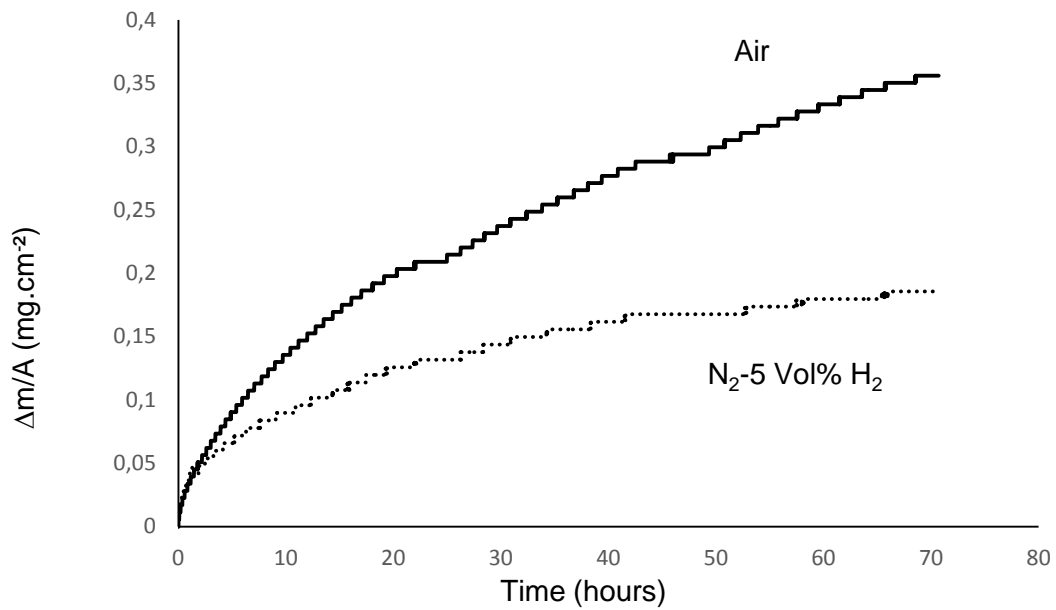


**Figure 1.** Mass gain versus time curves of FeCrSi alloy at 900 °C, in air and in N<sub>2</sub>-5 vol% H<sub>2</sub>

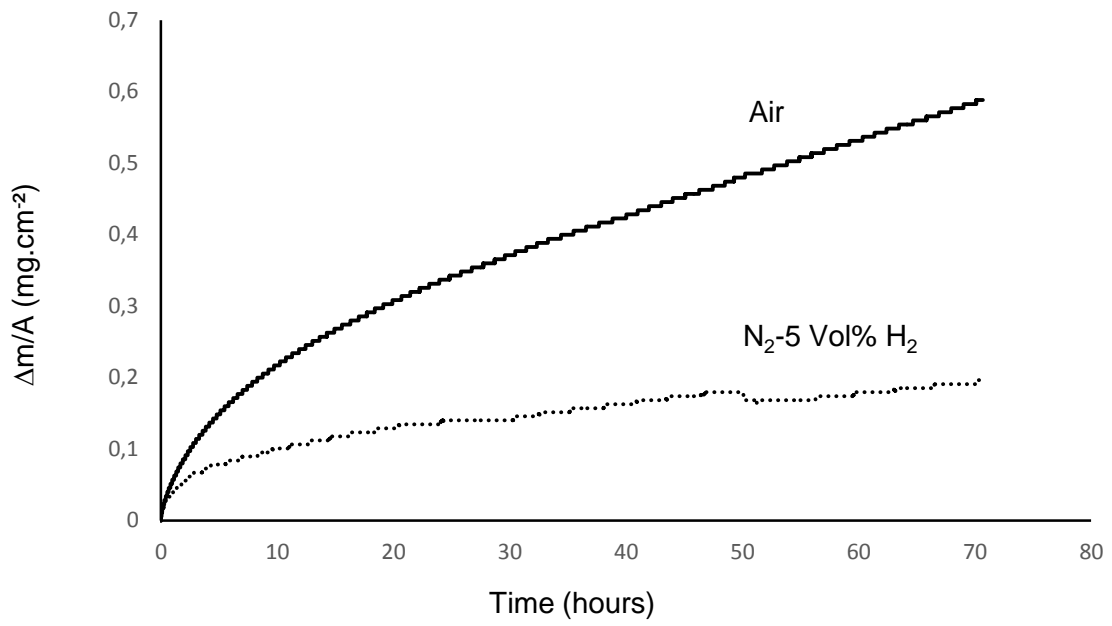


**Figure 2.** Mass gain versus time curves of FeCrSi alloy at 950 °C, in air and in N<sub>2</sub>-5 vol% H<sub>2</sub>

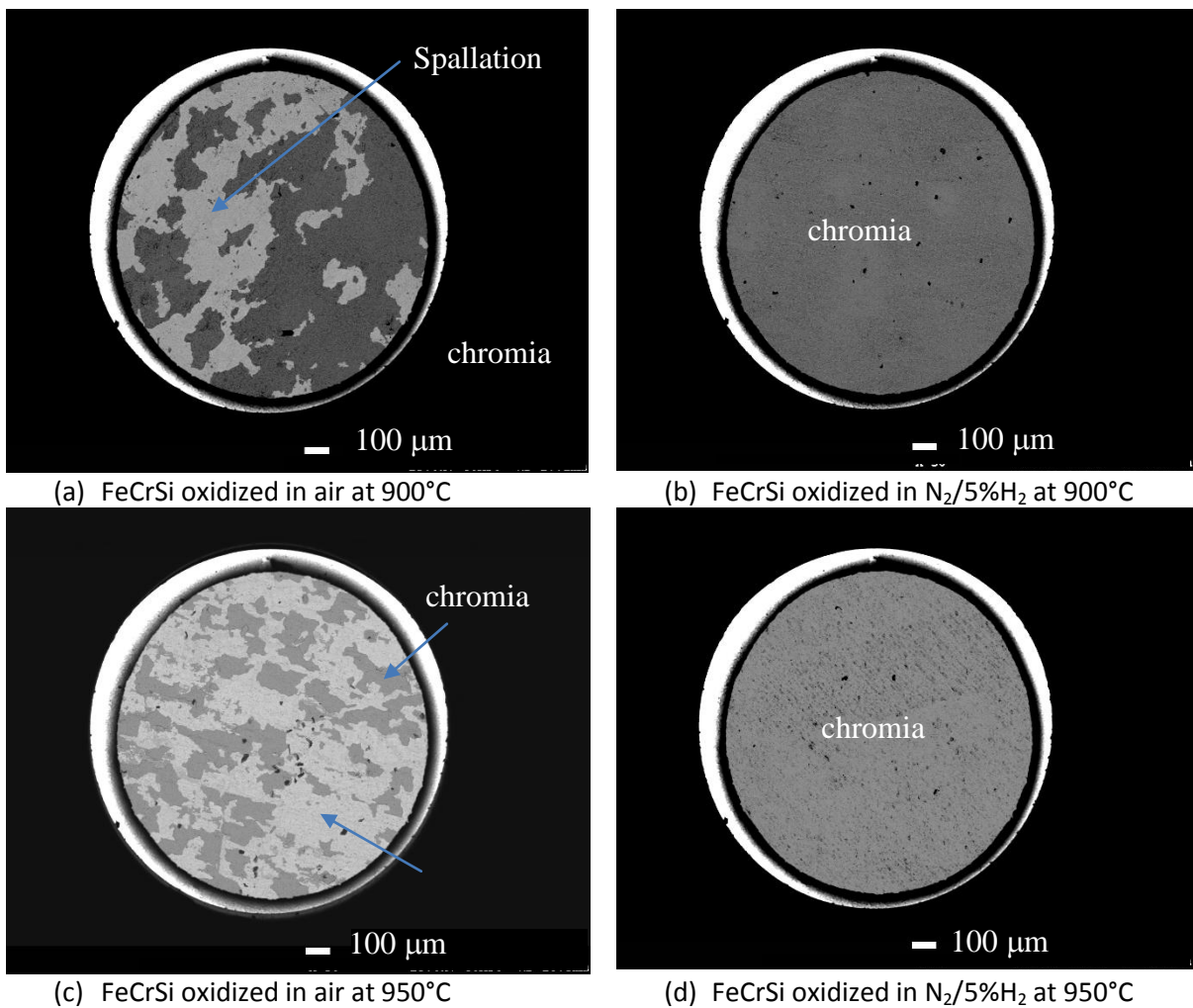
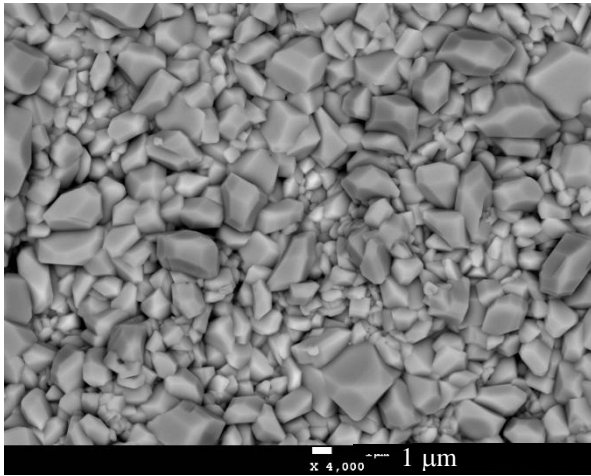
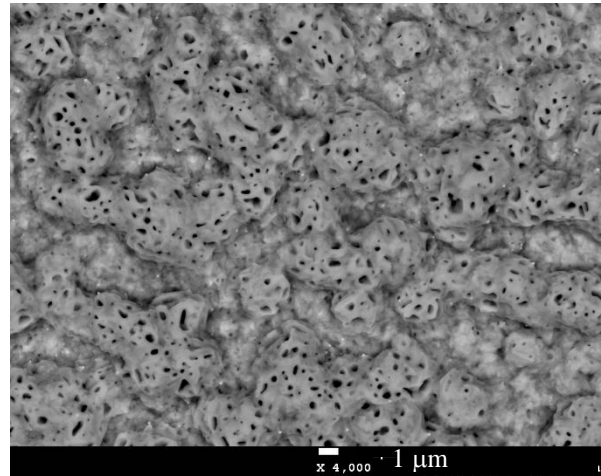


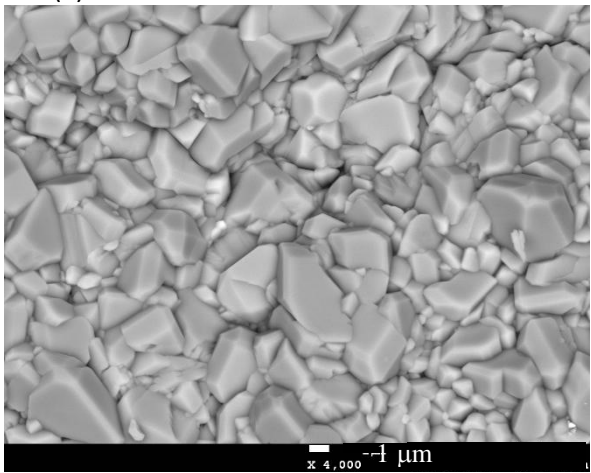
**Figure 3.** BSE images of samples surfaces (x50)



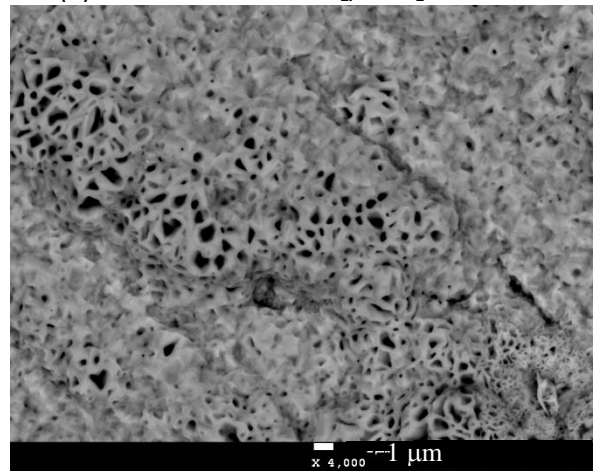
(a) FeCrSi oxidized in air at 900°C



(b) FeCrSi oxidized in N<sub>2</sub>/5%H<sub>2</sub> at 900°C

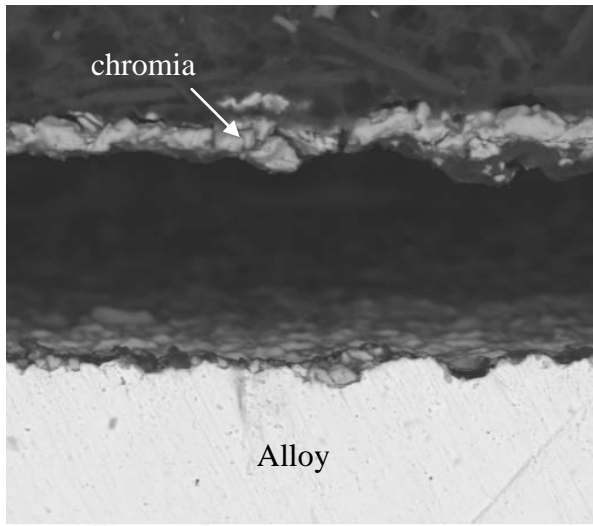


(c) FeCrSi oxidized in air at 950°C

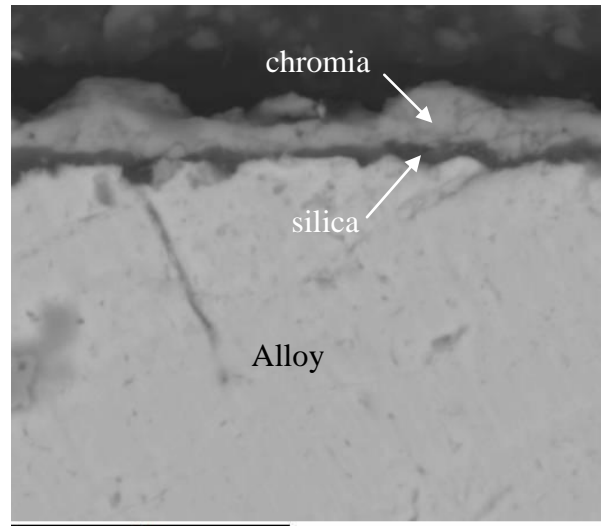


(d) FeCrSi oxidized in N<sub>2</sub>/5%H<sub>2</sub> at 950°C

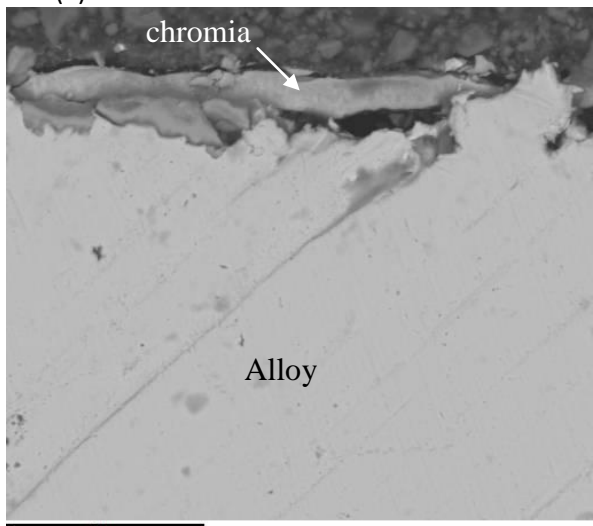
**Figure 4.** SEM observations of samples surfaces (x4000)



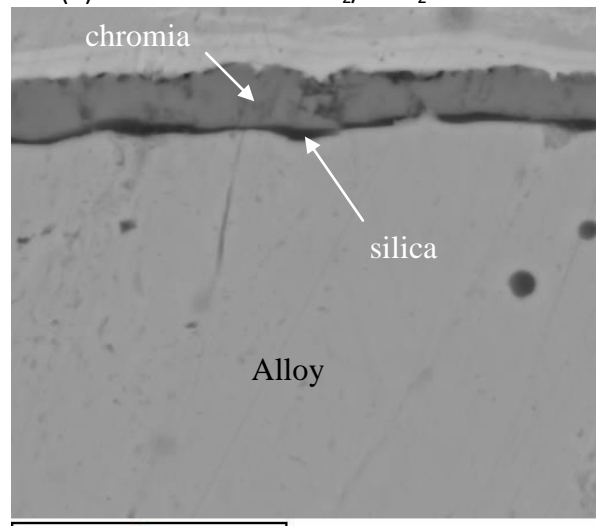
(a) FeCrSi oxidized in air at 900°C



(b) FeCrSi oxidized in N<sub>2</sub>/5%H<sub>2</sub> at 900°C



(c) FeCrSi oxidized in air at 950°C



(d) FeCrSi oxidized in N<sub>2</sub>/5%H<sub>2</sub> at 950°C

**Figure 5.** SEM observations of samples cross sections (b) and (d) : x4000 ; (a) and (c) : x1000

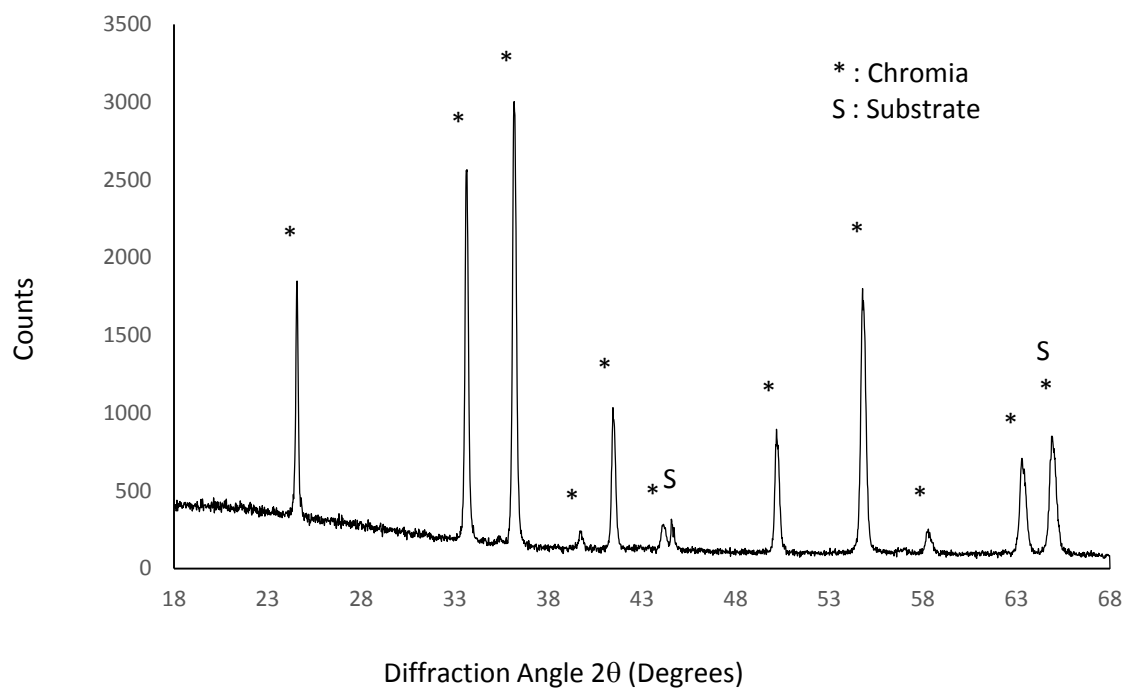


**Figure 6.** XRD patterns obtained on FeCrSi alloy after 70 h oxidation in N<sub>2</sub>-5 vol% H<sub>2</sub>